Adsorption of cysteine on TiO$_2$ at different pH values: Surface complexes characterization by FTIR-ATR and Langmuir isotherms analysis

S. Begonja[a], L.A. García Rodenas[b,c], E.B. Borghi[a], P.J. Morando[b,c,d,*]

[a] Universidad Nacional de Luján, Rutas 5 y 7, Buenos Aires, Argentina
[b] Gerencia de Química, Centro Atómico Constituyentes, Comisión Nacional de Energía Atómica, Avenida General Paz 1499, 1650 San Martín, Pcia. de Buenos Aires, Argentina
[c] Instituto de Tecnología Prof. J. Sábato, Universidad Nacional de General San Martín, Buenos Aires, Argentina
[d] Consejo Nacional de Investigaciones Científicas y Técnicas, Argentina

ABSTRACT

Surface complexes of cysteine amino acid onto TiO$_2$ films at pH 2.0, 5.0 and 8.0 were characterized by IR spectroscopy. The FTIR spectra at pH 2.0 show the coexistence of surface complexes with protonated and deprotonated carboxylate groups. This points to the occurrence of electrostatic interactions between the zwitterionic form of cysteine and the positively charged TiO$_2$ film. A Langmuir isotherm analysis was performed to obtain the binding constants values, which are consistent with electrostatically adsorbed surface species. At pH 8.0, the TiO$_2$ film is charged negatively, and the amino acid molecules approach the TiO$_2$ surface through the amino protonated groups. This new arrangement generates a larger surface concentration at saturation coverage.

© 2012 Elsevier B.V. All rights reserved.

1. Introduction

Cysteine is an amino acid commonly found in many proteins and enzymes, playing an essential role in many biochemical and pharmacological redox reactions. Several of these reactions have been studied 'in vivo' [1–6], where it is more difficult to obtain the reaction parameters, and 'in vitro' [7,8] in a homogeneous solution [9,10].

In aqueous solutions, the functional groups of the amino acids are available to undergo possible chemical reactions. However, if some of them are linked to an inorganic holder in an adequate way, the resulting framework may be used as a protein model. Its characterization would allow for a useful understanding of the different reactions that take place in "in vivo" conditions.

Furthermore, titanium implants are often used in dentistry and medicine [11]. Titanium is recovered by an inert thin layer of TiO$_2$ and, in the case of implants, this surface is in contact with different physiological fluids.

Adsorption of biomolecules on implant surfaces is an important phenomenon regarding the biocompatibility of prostheses and osseointegration process [12].

Adsorption of carboxylic acids [13–16], amino acids [17–21] and polyamino acids [22] on metal oxides has been reported in a large number of publications. Most previous works suggest that amino acids bind to metallic surface atoms through different functional groups. Jang and Condrate [17] investigated the adsorption of lysine to cation-substituted montmorillonites using infrared spectroscopy. They concluded that bidentate coordination occurred through the amino and carboxylic acid groups. Okazaki et al. [18] proposed that the adsorption of lysine to TiO$_2$ occurred *via* coordination of the amino group. However, in an infrared spectroscopy study of the adsorption of lysine on TiO$_2$ from an aqueous solution, Roddick-Lanzillotta et al. [19] conclude that at pH ≈ 5–7 there is no experimental evidence of lysine acting as ligand to surface Ti(IV) ions. They suggest that lysine accumulation on TiO$_2$ arises from electrostatic interactions between cationic amino acid and an anionic film. Martra et al. [20] indicated that the amino acid α-alanine is bound to TiO$_2$ surface in its zwitterionic form and that the adsorption strongly depends on the pH of the aqueous medium. In another paper Roddick-Lanzillotta et al. [22] analyze the influence of the electrostatic interactions of the polylysine with the adsorbent TiO$_2$, and reported that these interactions are very important to the adsorption process.

Concerning the adsorption of mercapto-carboxylic acids, in a recent paper Roncaroli et al. [23] studied the adsorption of thioglycolic acid onto a titanium dioxide sample at pH 4, using ATR-FTIR spectroscopy. The authors suggested that the carboxylate plays a more important role than the −SH group in the adsorption

* Corresponding author at: Gerencia de Química, Centro Atómico Constituyentes, Comisión Nacional de Energía Atómica, Avenida General Paz 1499, 1650 San Martín, Pcia. de Buenos Aires, Argentina. Tel.: +54 11 6772 7176; fax: +54 11 6772 7886.
E-mail address: morando@cnea.gov.ar (P.J. Morando).

processes. Two adsorption isotherms are required in order to explain the spectral data, even though only one spectral component is found. The adsorption of thioglycolic acid on CdS thin films has been studied by Young et al. [24]. In this case, based on the absence of the band corresponding to S—H stretching in the infrared spectrum, the authors postulate that the adsorption occurs *via* the deprotonated thiol group.

The cysteine adsorption on metallic surfaces has been studied through ultrahigh vacuum (UHV) techniques. Most previous papers [25–29] are about the bonding to the metal in the form of a thiolate, and the structure of monolayers deposited onto clean and ordered metal (Au, Pt, Cu) or metal oxide surfaces. The carboxylate group may play an important role in the bonding of cysteine on the TiO_2 surface [30]. Ataman et al. [31] studied the adsorption of cysteine on a rutile TiO_2 surface in UHV conditions, and the results show that the molecules bind to the Ti atoms through the carboxylic groups, and the majority of all thiol groups do not participate in the adsorption process.

The surface specific analytical tools used in UHV experiments are not applicable in wet environments [21]. Therefore, there is not much information on the cysteine adsorption processes on a TiO_2 surface in wet environments. For example, Rajh et al. [32] report a study about the surface modification of small particles of TiO_2 colloids with an aqueous solution of 0.1 M cysteine at pH 4. The results obtained by infrared spectroscopy suggest that the carboxyl group is involved in the binding of cysteine on the TiO_2 surface. However, the stretching vibration of the SH group was not affected by adsorption.

For a better understanding of the interfacial biological molecule/titanium dioxide interactions, we have studied the adsorption of cysteine aqueous solutions on TiO_2 film at pH 2.0, 5.0 and 8.0. The characterization of the surface complexes was carried out by attenuated total reflection (ATR) spectroscopy. The ATR mode allows for the exploration of the interfacial region with minimum interference from the dissolved species. The binding constants for cysteine adsorption on TiO_2 at the mentioned pH values were obtained from conventional adsorption isotherm experiments. The nature of the adsorption was discussed, taking into account the pH spectral dependence, and the binding constants were calculated by applying the Langmuir isotherm model.

2. Materials and methods

Titanium dioxide, Degussa P-25, has a particle size of *ca.* 25 nm. Its BET specific surface area is $51.4 \, m^2 \, g^{-1}$ and was determined from N_2 adsorption at 77 K. The sample is mainly anatase and the content of rutile is less than *ca.* 20%. Suspensions were prepared with bidistilled water and were aged for 15 days.

The cysteine amino acid, as cysteine hydrochloride dihydrate (Fluka) ($C_3H_7NO_2S \cdot ClH \cdot 2H_2O$), was at analytical grade and used without further purification.

FTIR spectra were recorded using a NICOLET 560 instrument equipped with a liquid N_2 cooled MCT-A detector. A horizontal ZnSe-ATR unit (area = 10 mm × 72 mm) was used; the incidence angle was 45° and total number of reflections was 11. This ATR element was SpectraTech.

Layers of TiO_2 particles were deposited by placing 200 μl of TiO_2 suspensions (6 g dm^{-3}) on the surface of the ATR crystal and evaporated to dryness at room temperature. The coated crystal was mounted in an ATR cell, and was allowed to equilibrate with a ligand-free solution until the FTIR signal became stable, and a blank single-beam spectrum was collected. Then, the oxygen-free solution of cysteine was added, and the IR-absorption spectra were recorded at 5–10 min intervals until signal amplitudes reached stable values. The working temperature was $25 \pm 2 \, °C$. Spectral
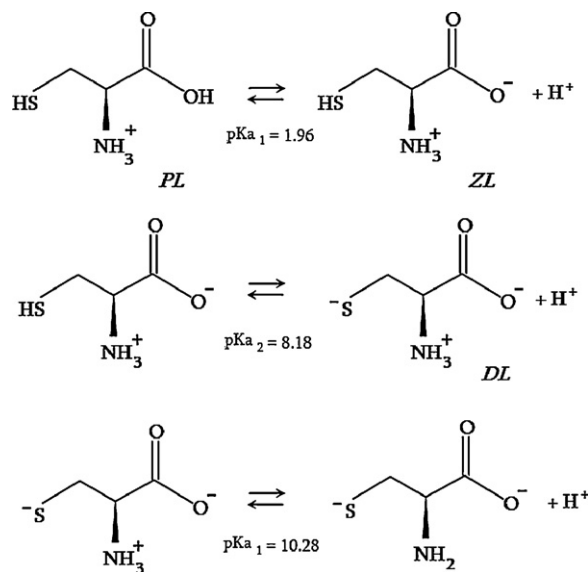

Fig. 1. Summary of pK_a of predominant cysteine species [34].

resolution was 2 cm^{-1}. Each of the final spectra is the average of 256 scans. Base line corrections were made in order to eliminate minor fluctuations due to instrumental instabilities. Under these conditions, since the cysteine concentration was always below *ca.* $1 \times 10^{-3} \, mol \, dm^{-3}$, no appreciable IR signal was detected from solution species. The FTIR-ATR spectra of free cysteine solutions of about 0.2 mol dm^{-3} were recorded as before.

The solutions at pH 2.0 were measured initially on a germanium crystal, but the absorbances were decreased relative to ZnSe. Therefore, spectra were recorded on a ZnSe crystal in the shortest time possible, in order to minimize the possible dissolution process of this crystal at pH 2.0. It should be noted that the spectra recorded with both materials were very similar, except for the much greater sensitivity in the case of that recorded on ZnSe.

For adsorption isotherms measurements, 25.0 cm^3 of TiO_2 suspension (20 g dm^{-3}) at adequate pH, was mixed with increasing concentrations of cysteine solutions of the same volume and pH. This was controlled by adding concentrated solutions of HCl or NaOH to the suspensions and to the cysteine solutions, as required.

The experiments were performed under N_2 atmosphere in a magnetically stirred vessel immersed in a thermostat at $15.0 \pm 0.1 \, °C$, in darkness conditions. The equilibration time was about 90 min. Under these conditions, the concentration of the free ligand became constant. Samples were taken and filtered through a 0.45 μm cellulose acetate membrane. Cysteine concentration in the filtrate was measured spectrophotometrically using the Ellman method [33], involving the reaction of 5,5′-dithio-bis-(2-nitrobenzoic acid) (DTNB; $C_4H_8N_2O_8S_2$) with the thiol groups. 5.0 cm^3 of 0.1 mol dm^{-3} buffer phosphate at pH 8.0, EDTA 1×10^{-3} mol dm^{-3} and 0.100 cm^3 of DTNB (4 mg cm^{-3}) were added to the filtrated solution. The samples were measured after 15 min at a wavelength of 412 nm.

Cysteine blanks demonstrated that the amino acid concentration remains constant, showing that the oxidation is negligible in the experimental conditions.

3. Results and discussion

The overall charge of cysteine varies with the solution pH. Fig. 1 shows the predominant species present from pH 0 to 14 [34]: the fully protonated PL, the zwitterionic ZL, the thiol deprotonated DL and the amino deprotonated forms.
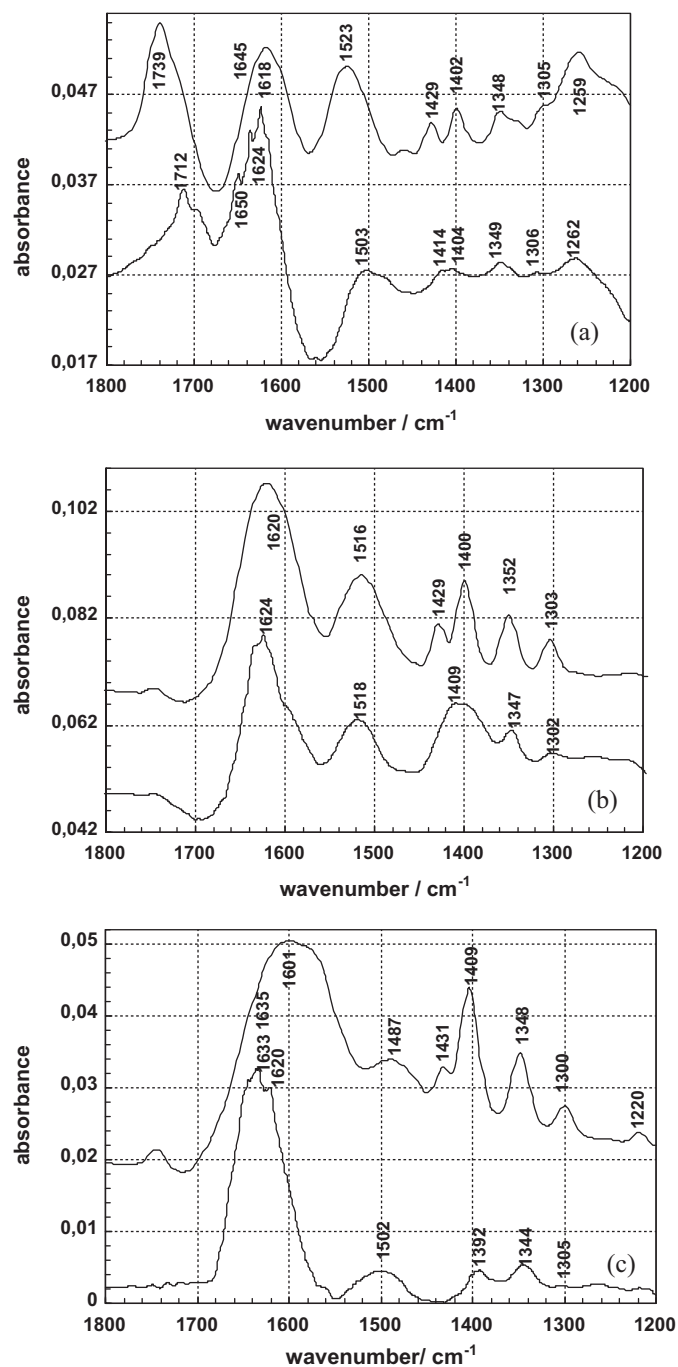
Fig. 2. ATR-FTIR spectra of 0.2 mol dm^{-3} cysteine solution (upper curves) and cysteine adsorbed to TiO$_2$ film from [cys] = 1 × 10^{-3} mol dm^{-3} (lower curves), at (a) pH 2.0, (b) pH 5.0 and (c) pH 8.0. The absorbance scale of solution spectra of (a) and (b) are offset by +0.008 and +0.05, respectively.

Cysteine can be bound to the metal surface *via* the carboxyl, amine and thiol groups and might form monodentate or bidentate surface complexes. It is well known that other amino acids, that do not contain a thiol group, form complexes with metal oxides in this way [17,18].

3.1. Comparative infrared spectra of cysteine in solution and adsorbed to TiO$_2$ at different pH values

Fig. 2 shows the ATR-FTIR spectra of 0.2 mol dm^{-3} cysteine solution and cysteine adsorbed to TiO$_2$ film from

[cys] = 1 × 10^{-3} mol dm^{-3}, at pH 2.0, 5.0 and 8.0. Tentative band assignments are summarized in Table 1 [16,19,20,35].

3.1.1. Spectra of cysteine solution

Fig. 2(a) illustrates the spectrum of free cysteine solution at pH 2.0. The bands centered at 1618 cm^{-1} and 1402 cm^{-1} are assigned to the antisymmetric and symmetric stretching modes of the carboxylate ion respectively, and two bands centered at 1739 cm^{-1} and 1259 cm^{-1} are ascribed to protonated carboxylate. These last two signals are assigned to the C=O and C—O stretches coupled with the OH in plane bend of the —COOH group, respectively [19]. It should be noted that the antisymmetrical bending band of the NH$_3^+$ group appears as a shoulder at 1645 cm^{-1} [35]. Therefore, the area of the bands at 1739 and 1618 cm^{-1}, is approximately consistent with the equimolar ratio of cysH$_3^+$ and cysH$_2$z species, predicted by the acid–base speciation expressions shown in Fig. 1.

At pH 5.0 (Fig. 2(b)), the bands centered at 1739 and 1259 cm^{-1} disappear, and the concomitant growing of the bands due to carboxylate ion at 1620 cm^{-1} and 1400 cm^{-1} can be seen. At this pH, the antisymmetrical bending band of the NH$_3^+$ group is overlapped with the antisymmetrical stretching band of the carboxylate ion. The main absorptions of the carboxylate ion and the symmetrical bending of the protonated amino group (1516 cm^{-1}), indicate that the amino acid is mainly in its fully zwitterionic form cysH$_2$z, and the pH dependence of the protonated and deprotonated carboxyl groups also varies as described in the acid–base speciation.

In the spectrum of the amino acid solution at pH 8.0, the bands ascribed to the antisymmetrical stretching of the carboxylate ion and antisymmetrical bending band of the NH$_3^+$ group are shifted regarding those present at pH 5.0. The symmetrical NH$_3^+$ bending band near 1523 cm^{-1} at pH 2.0 shifts to lower wavenumbers 1516 and 1487 cm^{-1} at pH 5.0 and 8.0, respectively.

The weak absorption band observed at pH 8.0 around 1220 cm^{-1} may arise and occur due to the scissoring of the H—N—C [35].

3.1.2. Spectra of cysteine adsorbed to TiO$_2$

Fig. 2 shows the infrared spectra of cysteine adsorbed to TiO$_2$. The bands appear quite similar to those for the amino acid in aqueous solution.

The tentative assignments for the main IR-absorption bands are summarized in Table 1. Literature data from Ref. [35] for cysteine in aqueous solution, and from Refs. [16,19,20] for other amino acids adsorbed on TiO$_2$ were used.

The spectrum of the cysteine adsorption to TiO$_2$ performed at pH 2.0 is a more complicated experiment (see Section 2), and the signals are less defined than those obtained at pH 5.0 and 8.0, especially between 1500 and 1200 cm^{-1}. However, its resemblance with that of the cysteine solution contributes to the band assignments. On the other hand, the absorption bands between 1800 and 1500 cm^{-1} are well defined and more relevant in order to study the interaction between the amino acid and the oxide surface. The coexistence of carboxylate groups in its protonated (1712 cm^{-1}) and deprotonated (1624 cm^{-1}) forms can be observed. It should be noted that the area of the first band is smaller than the second one, while in the solution species the area ratio between bands is close to 1.

In the IR spectrum of cysteine solution at pH 2.0, the antisymmetrical bending band of the NH$_3^+$ group appears as a slight shoulder at 1645 cm^{-1}. In the cysteine adsorbed to TiO$_2$ solution the slight shoulder is clearly more resolved at 1650 cm^{-1}. Roddick-Lanzillotta et al. [19] have reported that when lysine is fully in its protonated form at pH 0.9, the NH$_3^+$ antisymmetric deformation is completely resolved and the antisymmetric stretching mode of the carboxylate ion disappears. As can be seen in Fig. 2, for cysteine at

S. Begonja et al. / Colloids and Surfaces A: Physicochem. Eng. Aspects 403 (2012) 114–120

117

Table 1
Band assignments for the main IR-absorption bands of 0.2 mol dm^{-3} cysteine solutions and cysteine adsorbed on TiO$_2$ film from [cys] = 1.0 × 10^{-3} mol dm^{-3} solution, at pH 2.0, 5.0 and 8.0. Nomenclature: *vs, s, m, w, vw*: bands of very strong, strong, medium, weak and very weak intensities, respectively; *sh:* shoulder [16,19,20,23].

Assignment	pH 2.0		pH 5.0		pH 8.0	
	Cysteine	Cys on TiO$_2$	Cysteine	Cys on TiO$_2$	Cysteine	Cys on TiO$_2$
ν[C=O] + ν[O—H]	1739,*s*	1712,*m*				
δ_{as}[NH$_3{}^+$]bending	1645,*sh*	1650,*w*			1635,*sh*	1633,*w*
ν_{as}[CO$_2{}^-$]	1618,*s*	1624,*s*	1620,*vs*	1624,*vs*	1601,*vs*	1620,*vs*
δ_s[NH$_3{}^+$]bending	1523,*s*	1503,*m*	1516,*s*	1518,*s*	1487,*m*	1502,*m*
δ[CH$_2$]bending	1429,*w*	1414,*w*	1429,*w*		1431,*w*	
ν_s[CO$_2{}^-$]	1402,*w*	1404,*w*	1400,*m*	1409,*m*	1409,*s*	1392,*w*
δ[C—H]bending	1348,*m*	1349,*w*	1352,*m*	1347,*w*	1348,*m*	1344,*w*
w[CH$_2$]wagging	1305,*sh*	1306,*vw*	1303,*w*	1302,*vw*	1300,*w*	1305,*vw*
ν[C—O] + ν[O—H]	1259,*m*	1262,*w*				
β[HNC]scissoring					1220,*w*	

pH 2.0 the last band is still large and the band assigned to the NH$_3{}^+$ antisymmetric bending band appears clearly overlapped over it.

At pH 5.0, the infrared spectrum of cysteine adsorbed to TiO$_2$ is quite similar to those observed for the amino acid in aqueous solution, and Table 1 shows that the bands appear practically unchanged.

It can be seen that the spectrum at pH 8.0 exhibits at 1620 cm^{-1} the band ascribed to the deprotonated carboxylate function. The absorbance of the band at 1633 cm^{-1}, assigned to the NH$_3{}^+$ antisymmetric deformation, increases due to an absorption band arising from the bending mode of water. In effect, Roddick-Lanzillotta et al. [19] have indicated that the infrared spectrum of lysine adsorbed to TiO$_2$ at pH 12.6 shows an absorption band at 1650 cm^{-1}. This is due to incomplete background subtraction caused by the difference in ionic strength between the background solution and the strongly basic solutions. In the present case, the difference in ionic strength at pH 8.0 is not very large and, although a net band is not observed, this effect increases the absorbance of the NH$_3{}^+$ antisymmetric band.

Adsorption of carboxylic acids to different TiO$_2$ surfaces, under different experimental conditions, has been previously reported. The adsorption of a range of aliphatic mono- and di-carboxylic acids to metal oxides TiO$_2$, ZrO$_2$, Al$_2$O$_3$ and Ta$_2$O$_5$ has been investigated using *in situ* ATR-FTIR by Dobson and McQuillan [16]. These authors concluded that, for monocarboxylic acids, the adsorption occurs at the metal oxide surfaces through coordination *via* the carboxylate group. The absence of an absorption at ~1700 cm^{-1} indicates that adsorption to the metal oxides occurs as the completely deprotonated species. These authors analyzed the coordination modes (unidentate, chelating bidentate and bridging bidentate) from the differing separations between the antisymmetric (ν_{as}) and symmetric (ν_s) carboxylate stretch absorptions bands ($\Delta\nu$).

More recently, Capecchi et al. [36] and Ojamäe et al. [37] combined IR and quantum-chemical vibrational frequency calculations in order to understand the nature of the carbon–oxygen–titanium bonds. In particular, Capecchi et al. [36] observe the importance of the hydration and hydroxylation degrees of the surface and Ojamäe et al. [37] found that glycine was not adsorbed onto the rutile surface, possibly due to its interaction with the solvents used.

An infrared study of the adsorption of α-alanine on TiO$_2$ powder in aqueous suspension was carried out by Martra et al. [20] and the vibrational features of the carboxylate function of adsorbed L-Ala molecules suggested that this group assumes a bridged structure. Conversely, Roddick-Lanzillotta et al. [19] in a study about the adsorption of lysine to TiO$_2$ from an aqueous solution, concluded that there is no evidence for lysine coordination *via* a covalent bond and suggested that lysine accumulation on TiO$_2$ arises from electrostatic interactions. This is supported by a low binding constant obtained from adsorption isotherm experiments. Consistent with this result, Langel and Menken [38] in a simulation by first

principles molecular dynamics of the amino acids adsorption, conclude that in solution the adhesion is driven by weaker interactions than those obtained by UHV techniques. The data suggest that different mechanisms account for adsorption in UHV and in solution; therefore, their respective spectra cannot be compared. This weak adhesion in solution can be due to electrostatic interaction or to hydrogen bonding.

Our results also propose that cysteine is electrostatically adsorbed on TiO$_2$. At pH 2.0, the adsorption band arising from the carboxylate group in its protonated form is observed at 1712 cm^{-1}. Therefore, in opposition to the study performed by Dobson and McQuillan [16] referred to the adsorption of aliphatic mono-carboxylic acids to TiO$_2$ from aqueous solutions, the surface coordination also occurs *via* the protonated cysteine form. The observation of a large absorption band arising from the carbonyl stretch of the carboxylic acid is only possible if favorable electrostatic interactions between highly positively charged TiO$_2$ surface at pH 2.0 (TiO$_2$ exhibits a point of zero charge at pH ~6.5 [39]) and the high electronic density moiety of the —COOH group, or if hydrogen bonds are formed.

On the other hand, in the spectra of cysteine solution the area of the bands corresponding to the ν[CO$_2$H] and ν_{as}[CO$_2{}^-$] is quite similar, in agreement with the equimolar ratio of the fully protonated and zwitterionic forms, respectively, as predicted by the acid–base speciation at this pH value. But in the spectra of a TiO$_2$ film in contact with cysteine, the area of the protonated form is smaller. This fact can be attributed to the more favorable electrostatic interactions between TiO$_2$ (with a net positive surface charge) and the anionic group —COO$^-$, with regard to the polar group —COOH.

At pH 5.0 the cysteine is adsorbed in the zwitterionic form and the spectrum resembles strongly that of dissolved species. The absence of the ~1712 cm^{-1} band indicates that the surface coordination occurs through the completely deprotonated carboxylate species.

The differing separation between the carboxylate stretch absorption bands $\Delta\nu$ for the adsorbed species are 220 and 215 cm^{-1} at pH 2.0 and 5.0, respectively. Although these magnitudes of $\Delta\nu$ do not agree exactly with the band separations analyzed by Dobson and McQuillan [16], they are close to that of the bridging bidentate coordination mode ($\Delta\nu$ = 150–180 cm^{-1}). However, the small difference in the separation between $\Delta\nu$ of the adsorbed species ($\Delta\nu_{ads}$) and that of the free species ($\Delta\nu_{free}$) at pH 2.0 and 5.0 proves the scanty interaction between the oxide surface and the amino acid, and supports the idea that a chemical bond is not involved. As it can be seen in the next section, the binding constants for cysteine adsorption to TiO$_2$ calculated by applying the Langmuir isotherm model support this hypothesis.

At pH 8.0, the TiO$_2$ surface exhibits a net negative charge and the carboxylate group would be electrostatically repelled from
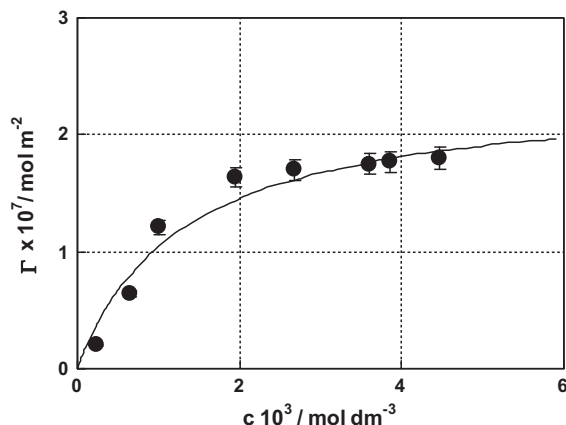
Fig. 3. Adsorption isotherms of cysteine on titanium dioxide at pH 5.0 and 15 °C. Data have been fitted according to Eq. (1). The experimental values are the average of three determinations, which differ by no more than 5%.
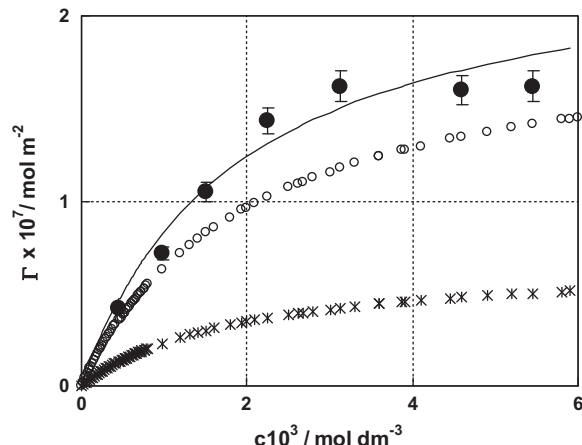

Fig. 4. Adsorption isotherms of cysteine on titanium dioxide at pH 2.0 and 15 °C. Data have been fitted according to Eq. (2). Dashed lines show the contributions of PL (○) and ZL (*) species (see text). The experimental values are the average of three determinations which differ by no more than 5%.

the surface. However, the separation between $\Delta \upsilon_{ads}$ and $\Delta \upsilon_{free}$, more than expected, would suggest a more effective interaction. Roddick-Lanzillotta et al. [22] also found a stronger peptide–TiO$_2$ interaction going from dilysine to trilysine at pH 7.4. These authors propose that it becomes more feasible for the carboxylate to approach the surface in an orientation suitable for binding, from the electrostatic interactions of the three side-chain amine groups with TiO$_2$. Consistent with this result was a larger than expected increase in the experimentally determined binding constants for trilysine, compared with lysine and dilysine.

In the present case, the binding constant obtained from isotherm experiments (see below) implies that the coordination of cysteine to TiO$_2$ *via* covalent bond formation does not occur. Therefore, a possible explanation is that the cysteine molecules approach the amino protonated groups to the negatively charged surface. The difference separation between $\Delta \upsilon_{ads}$ and $\Delta \upsilon_{free}$ may be due to the environmental changes of the carboxylate group produced by the molecule spatial reconformation.

3.2. Adsorption isotherms of cysteine on TiO$_2$

3.2.1. Adsorption isotherms of cysteine on TiO$_2$ at pH 5.0

Fig. 3 displays the adsorption isotherms at pH 5.0, where the amino acid is present in the zwitterionic form ZL. Assuming the adsorption follows the Langmuir isotherm, Eq. (1) can be derived:

$$\Gamma = \frac{\Gamma_{\max ZL} K_{ZL} C_{ZL}}{1 + K_{ZL} C_{ZL}} \tag{1}$$

where Γ is the surface concentration of cysteine in the zwitterionic form, $\Gamma_{\max ZL}$ and K_{ZL} are the surface concentration at saturation coverage and the equilibrium constant for the adsorption of ZL species respectively, and C_{ZL} is the equilibrium concentration. At this pH value, C_{ZL} is the analytical concentration. The solid line in Fig. 3 was obtained from Eq. (1) with K_{ZL} = 770 mol^{-1} dm^3 and $\Gamma_{\max ZL}$ = 2.4 × 10^{-7} mol m^{-2}.

This value of the binding constant is characteristic of electrostatic interactions. Indeed, typical binding constants values arising from electrostatic interactions are around 10^3 mol^{-1} dm^3 [40]. In agreement, Roddick-Lanzillotta et al. [19] suggest that electrostatic interactions between the cationic form of lysine and an anionic film of TiO$_2$ occur, starting from a low binding constant value of 3 × 10^3 mol^{-1} dm^3. Nevertheless, larger binding constants are consistent with covalent interactions ligand-adsorbent. For example, oxalate coordinated to TiO$_2$ (*via* a side-on bridging bidentate covalent interaction) exhibited binding constants of $K \approx 10^4$ mol^{-1} dm^3 [19].

The experimental values with their uncertainty bars are presented in Fig. 3. These are the average of three values which differ by no more than 5%. It should be noted that several uncertainty bars do not pass through the curve derived from the model. In order that these fall within the model predictions, the uncertainties should be increased to 10%. This deviation could indicate that the equilibrium constant K_L is actually a function of the surface coverage degree. The assumption is reasonable in the case of weak electrostatic interactions whose effect should decrease with increasing the surface coverage. Whereas the difference does not really affect the aim of the work, we have fitted the experimental values with the simple Langmuir model instead of adding a new parameter to it. The same fact is observed at the other pH values.

3.2.2. Adsorption isotherms of cysteine on TiO$_2$ at pH 2.0

A simple model of equilibrated competitive chemisorption for the fully protonated and the zwitterionic forms of cysteine, can be described by Eq. (2):

$$\Gamma = \frac{\Gamma_{\max PL} K_{PL} C_{PL}}{1 + K_{PL} C_{PL} + K_{ZL} C_{ZL}} + \frac{\Gamma_{\max ZL} K_{ZL} C_{ZL}}{1 + K_{ZL} C_{PL} + K_{ZL} C_{ZL}} \tag{2}$$

where $\Gamma_{\max PL}$ and K_{PL} are the surface concentration at saturation coverage and the equilibrium constant for the adsorption of the fully protonated PL species, respectively, and C_{PL} is the equilibrium concentration. The total adsorption isotherm of cysteine on TiO$_2$ is shown in Fig. 4, together with the contribution of PL and ZL species (depicted by the first and the second addends of Eq. (2)); it can be seen that the surface concentration at saturation coverage is similar to that of pH 5.0.

Titanium dioxide has a point of zero charge PZC = 6.5 [37]. Therefore, it could be assumed that the net surface charge is not appreciably modified between pH 2.0 and 5.0, and that the binding constant for the zwitterionic species does not change. From this assumption, a K_{PL} constant value of 197 mol^{-1} dm^3 and $\Gamma_{\max PL} = \Gamma_{\max ZL}$ = 2.4 × 10^{-7} mol m^{-2} can be calculated.

The solid line in Fig. 4 was obtained according to Eq. (2) and the dotted lines represent the adsorption contribution of the fully protonated PL and the zwitterionic ZL species. The concentrations of these species were calculated from the total cysteine equilibrium concentration and pK_{a1} value.

The lower value of K_{PL} indicates that at pH 2.0 the TiO$_2$ surface sites exhibit lower affinity for the PL form than for the ZL one, in agreement with the smaller area of the band at 1714 cm^{-1} (Fig. 2(a), lower curve). It should be noted that the equivalent bands in aqueous solution have almost the same area. As expected, the
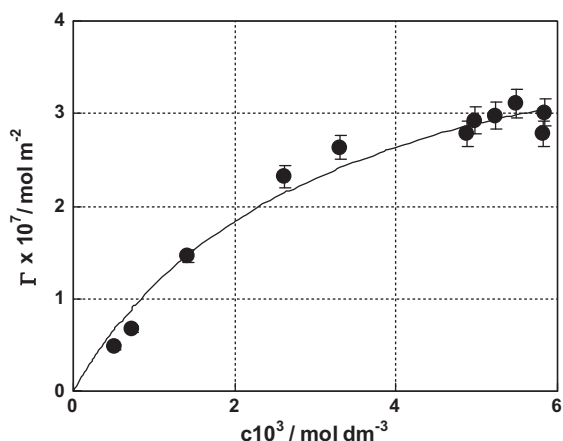
Fig. 5. Adsorption isotherms of cysteine on titanium dioxide at pH 8.0 and 15 °C. Data have been fitted according to Eq. (3). The experimental values are the average of three determinations which differ by no more than 5%.

overall charge of the fully protonated species results in a smaller electrostatic interaction with the cationic film of TiO$_2$.

An estimate of pK_{a1}(COOH) for adsorbed cysteine can be made from the equilibrium constants data for the adsorption of PL and ZL species. This value was determined to be 1.37. Therefore, adsorption of cysteine resulted in a pK_{a1}(COOH) decrease of 0.59. This reduction in the pK_a(COOH) value for a ligand after adsorption was also found for mercaptoacetic and mercaptopropionic acids adsorbed to CdS thin films [24].

3.2.3. Adsorption isotherms of cysteine on TiO$_2$ at pH 8.0

The adsorption isotherm is shown in Fig. 5. As can be seen at pH 2.0, a simple model of competitive chemisorption for the zwitterionic ZL and deprotonated thiolate DL forms can be described by an equation equivalent to (2):

$$\Gamma = \frac{\Gamma_{\max ZL} K_{ZL} C_{ZL}}{1 + K_{ZL} C_{ZL} + K_{DL} C_{DL}} + \frac{\Gamma_{\max DL} K_{DL} C_{DL}}{1 + K_{ZL} C_{ZL} + K_{DL} C_{DL}} \tag{3}$$

The solid line in Fig. 5 was obtained from Eq. (3) with $K_{ZL} = 305$ mol^{-1} dm^3, $K_{DL} = 380$ mol^{-1} dm^3, and $\Gamma_{\max ZL} = \Gamma_{\max DL} = 4.5 \times 10^{-7}$ mol m^{-2}. A good fitting of the experimental values can also be carried out using Eq. (1), with $K = 350$ mol^{-1} dm^3 and $\Gamma_{\max} = 4.5 \times 10^{-7}$ mol m^{-2}.

The stretching vibrational mode of the thiol group, centered at 2550 cm^{-1} [41], is not observed in the recorded spectra shown in Fig. 2. Therefore, the FTIR spectroscopy is unable to determine the abundance ratio of ZL and DL species adsorbed at pH 8.0.

On the other hand, the surface concentration at saturation coverage at pH 8.0 is larger than at pH 2.0 and 5.0, and the TiO$_2$ surface exhibits a net negative charge (point of zero charge for TiO$_2$: PZC = 6.5). Therefore, Coulombic electrostatic attractions explain that the approach of the side-chain amino protonated groups to the negatively charged surface would be an orientation suitable for the cysteine molecules. In this arrangement, the thiolate groups extend into the solution in a way that provides for a better use of the superficial space and a larger $\Gamma_{\max}$ value.

A schematic representation of the possible configuration of cysteine adsorbed on TiO$_2$ at pH 5 and 8 is shown in Fig. 6. As can be seen, the thiol side chain would have little interaction with the TiO$_2$ surface at pH 8 and its ionization status would not influence the adsorption process. The spatial layout that the molecules acquire, approaches the partially deprotonated thiol —SH to the carboxylate —COO$^-$ group. This modification in the environment of the carboxylate may contribute to the spectral changes shown by this group.
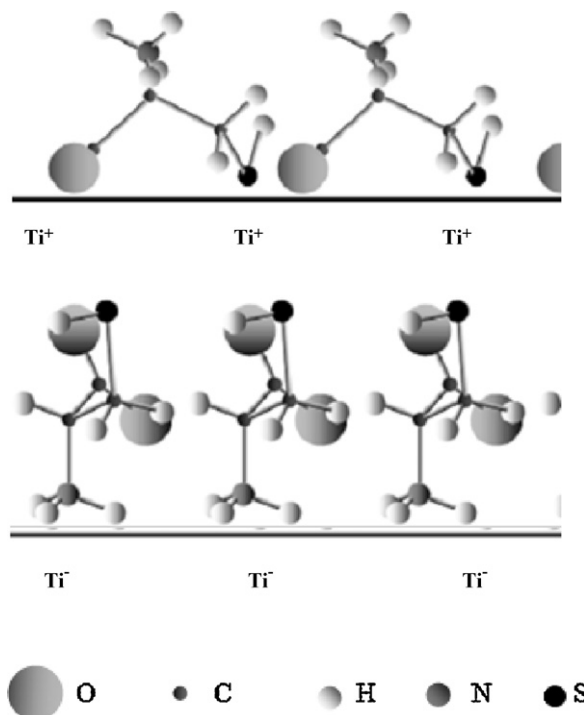

Fig. 6. Schematic representation of possible cysteine coordination to TiO$_2$ at pH 5.0 (upper) and 8.0 (lower).

Therefore, the cysteine coordination to TiO$_2$ would be consistent with the idea of two undistinguishable species with $K_L = 350$ mol^{-1} dm^3.

4. Conclusions

Infrared studies revealed that cysteine is adsorbed on TiO$_2$ from aqueous solutions at pH 2.0–8.0. Binding constants were calculated by applying the Langmuir isotherm model, and their values are consistent with an electrostatically adsorbed surface species. Under these conditions, there is no evidence for cysteine acting as chemical bond to surface Ti(IV) ions. The adsorption is pH-dependent: the overall charge of cysteine and the surface charge density of TiO$_2$ vary with the solution pH. This fact is demonstrated by the internal reflection infrared spectroscopic study and the Langmuir isotherm analysis.

At pH 2.0, cysteine is adsorbed mainly in the fully protonated and zwitterionic forms. The fittings obtained from adsorption isotherm experiments suggest a competitive adsorption of these species onto the TiO$_2$ surface sites, but the zwitterionic form shows more affinity. This is supported by a major accumulation of this species on TiO$_2$, reflected by the absorbance ratio of the respective bands.

Adsorption of cysteine produces a decrease in pK_{a1}(COOH) value from 1.96 to 1.37.

At pH 5.0, the amino acid is in the zwitterionic form. This fact is consistent with the FTIR spectrum and the adsorption isotherms obtained.

At pH 8.0, there are favorable electrostatic interactions between the highly negatively charged TiO$_2$ surface and the protonated amine parts of cysteine, while the carboxylate and thiolate groups are electrostatically repelled from the surface. Therefore, the amino groups approach the surface, which causes the other groups to extend into the solution. There is a larger adsorption density at saturation coverage due to the spatial layout of the cysteine attached on the TiO$_2$ surface.

Acknowledgements

References

[1] T. Nishi, N. Shimizu, M. Hiramoto, I. Sato, Y. Yamaguchi, M. Hasegawa, S. Aizawa, H. Tanaka, K. Kataoka, H. Watanabe, H. Handa, Spatial redox regulation of a critical cysteine residue of NF-B *in vivo*, J. Biol. Chem. 277 (2002) 44548–44556.

[2] C.K. Sen, Cellular thiols and redox-regulated signal transduction, Curr. Top. Cell. Regul. 36 (2001) 151–180.

[3] A. Salmeen, D. Barford, Functions and mechanisms of redox regulation of cysteine-based phosphatases, Antioxid. Redox Signal. 7 (5–6) (2005) 560–577.

[4] L.M. Hicks, R.E. Cahoon, E.R. Bonner, R.S. Rivard, J. Sheffield, J.M. Jez, Thiol-based regulation of redox-active glutamate–cysteine ligase from *Arabidopsis thaliana*, Plant Cell 19 (2007) 2653–2661.

[5] W. Maret, B.L. Vallee, Thiolate ligands in metallothionein confer redox activity on zinc clusters, Proc. Natl. Acad. Sci. U.S.A. 95 (7) (1998) 3478–3482.

[6] R. Barnejee, Redox Biochemistry, John Wiley & Sons, 2007.

[7] R.J. Turner, J.H. Weiner, D.E. Taylor, Selenium metabolism in *Escherichia coli*, Biometals 11 (1998) 223–227.

[8] H.E. Ganther, Selenium metabolism, selenoproteins and mechanisms of cancer prevention: complexities with thioreductase, Carcinogenesis 20 (9) (1999) 1657–1666.

[9] J.L. Kice, T.W.S. Lee, S. Pan, Mechanism of the reaction on thiols with selenite, J. Am. Chem. Soc. 102 (1980) 4448–4455.

[10] D.O. Forastiere, E.B. Borghi, P.J. Morando, Reaction mechanism of selenate(IV) ion with several thiols in aqueous media, Helv. Chim. Acta 90 (2007) 1152–1159.

[11] A. Schroeder, F. Sutter, D. Buser, G. Krekeler, Oral Implantology, Thieme Medical Publishers, New York, 1996.

[12] A. Welle, M. Grunze, D. Tur, Plasma protein adsorption and platelet adhesion on poly[bis(trifluoroethoxy)phosphazene] and reference material surfaces, J. Colloid Interface Sci. 197 (1998) 263–274.

[13] S. Hug, B. Sulzberger, *In situ* Fourier transform infrared: spectroscopic evidence for the formation of several different surface complexes of oxalate on TiO$_2$ in the aqueous phase, Langmuir 10 (1994) 3587–3597.

[14] K.D. Dobson, P.A. Connors, A.J. McQuillan, Monitoring hydrous metal oxide surface charge and adsorption by STIRS, Langmuir 13 (1997) 2614–2616.

[15] T. Awatani, K.D. Dobson, A.J. McQuillan, B. Ohtani, K. Uozaki, *In situ* infrared spectroscopic studies of adsorption of lactic acid and related compounds on the TiO$_2$ and CdS semiconductor photocatalyst surfaces from aqueous solutions, Chem. Lett. (1998) 849–850.

[16] K.D. Dobson, A.J. Mc Quillian, *In situ* infrared spectroscopic analysis of the adsorption of aliphatic carboxylic acids to TiO$_2$, ZrO$_2$, Al$_2$O$_3$, and Ta$_2$O$_5$ from aqueous solutions, Spectrochim. Acta Part A 55 (1999) 1395–1405.

[17] S.D. Jang, R.A. Condrate, The IR spectra of lysine adsorbed on several cation-substituted montmorillonites, Clays Clay Miner. 20 (1972) 79–82.

[18] S. Okazaki, T. Aoki, K. Tani, Adsorption of basic α-amino acids in an aqueous solution by titanium(IV) oxide, Bull Chem. Soc. Jpn. 54 (1981) 1595–1599.

[19] A.D. Roddick-Lanzillotta, P.A. Connors, A.J. Mc Quillian, An *in situ* infrared spectroscopic study of the adsorption of lysine to TiO$_2$ from an aqueous solution, Langmuir 14 (1998) 6479–6484.

[20] G. Martra, S. Horikoshi, M. Anpo, S. Coluccia, H. Hidaka, FTIR study of adsorption and photodegradation of L-α-alanine on TiO$_2$ powder, Res. Chem. Intermed. 28 (2002) 359–371.

[21] Z. Pászti, T. Quezthelyi, O. Hakkel, L. Guczi, Adsorption of amino acids on hydrophilic surfaces, J. Phys.: Condens. Matter 20 (2008) 224014–224020.

[22] A.D. Roddick-Lanzillotta, A.J. Mc Quillan, An *in situ* infrared spectroscopic investigation of lysine peptide and polylysine adsorption to TiO$_2$ from aqueous solutions, J. Colloid Interface Sci. 217 (1999) 194–202.

[23] F. Roncaroli, P.Z. Araujo, P.J. Morando, A.E. Regazzoni, M.A. Blesa, FTIR/ATR characterization of TiO$_2$/aqueous solution interfaces, in: P. Birkle, I.S. Torres-Alvarado (Eds.), Water–Rock Interaction, CRC Press, Boca Raton, FL, 2010, pp. 41–46.

[24] A.G. Young, D.P. Green, A.J. McQuillan, Infrared spectroscopic studies of monothiol ligand adsorption on CdS nanocrystal films in aqueous solutions, Langmuir 22 (2006) 11106–11112.

[25] G. Dodero, L. DeMichieli, O. Cavalleri, R. Rolandi, L. Oliveri, A. Daccà, R. Parodi, L-Cysteine chemisorption on gold: an XPS and STM study, Colloids Surf. A 175 (2000) 121–128.

[26] O. Cavalleri, G. Gonella, S. Terreni, M. Vignolo, P. Pelori, L. Floreano, A. Morgante, M. Cánepa, R. Rolandi, High resolution XPS of the S 2p core level region of the L-cysteine/gold interface, J. Phys.: Condens. Matter 16 (2004) S2477–S2482.

[27] A.P.J. Stampfl, C.-H. Chen, S.-C. Wang, M.-L. Huang, R. Klauser, A scanning photoemission microprobe study of the adsorption of cysteine on Pt{1 1 1}, J. Electron. Spectrosc. Relat. Phenom. 144–147 (2005) 417–420.

[28] G. Gonella, S. Terreni, D. Cvetko, A. Cossaro, L. Mattera, O. Cavalleri, R. Rolandi, A. Morgante, L. Floreano, M. Cánepa, Ultrahigh vacuum deposition of L-cysteine on Au(1 1 0) studied by high-resolution X-ray photoemission: from early stages of adsorption to molecular organization, J. Phys. Chem. B 109 (2005) 18003–18009.

[29] J.W. Kim, H.-N. Hwang, C.-C. Hwang, Adsorption of cysteine on Cu(1 1 0) studied by core-level photoelectron spectroscopy, J. Phys. Chem. C 111 (2007) 13192–13196.

[30] L. Thomsen, M.T. Wharmby, D.P. Riley, G. Held, M.J. Gladys, The adsorption and stability of sulfur containing amino acids on Cu{5 3 1}, Surf. Sci. 603 (2009) 1253–1261.

[31] E. Ataman, C. Isvoranu, J. Knudsen, K. Schulte, J.N. Andersen, J. Schnadt, Adsorption of L-cysteine on rutile TiO$_2$ (1 1 0), Surf. Sci. 605 (2011) 179–186.

[32] T. Rajh, A.E. Ostafin, O.I. Micic, D.M. Tiede, M.C. Thurnauer, Surface modification of small particle TiO$_2$ colloids with cysteine for enhanced photochemical reduction: an EPR study, J. Phys. Chem. 100 (1996) 4538–4545.

[33] G.L. Ellman, Tissue sulfhydryl groups, Arch. Biochem. Biophys. 82 (1959) 70–77.

[34] J.G. Speight (Ed.), Lange's Handbook of Chemistry, 16th ed., McGraw Hill Standar Handbooks, 2005, p. 4.157.

[35] M. Wolpert, P. Hellwig, Infrared spectra and molar absorption coefficients of the 20 alpha amino acids in aqueous solutions in the spectral range from 1800 to 500 cm^{-1}, Spectrochim. Acta A 64 (2006) 987–1001.

[36] G. Capecchi, M.G. Faga, G. Martra, S. Coluccia, M.F. Iozzi, M. Cossi, Adsorption of CH$_3$COOH on TiO$_2$: IR and theoretical investigations, Res. Chem. Intermed. 33 (2007) 269–284.

[37] L. Ojamäe, C. Aulin, H. Pedersen, P.-O. Käll, IR and quantum-chemical studies of carboxylic acid and glycine adsorption on rutile TiO$_2$ nanoparticles, J. Colloid Interface Sci. 296 (2006) 71–78.

[38] W. Langel, L. Menken, Simulation of the interface between titanium oxide and amino acids in solution by first principles MD, Surf. Sci. 538 (2003) 1–9.

[39] R. Rodríguez, M.A. Blesa, A.E. Regazzoni, Surface complexation at the TiO$_2$ (anatase)/aqueous solution interface: chemisorption of catechol, J. Colloid Interface Sci. 177 (1996) 122–131.

[40] K.D. Dobson, A.J. McQuillan, An infrared spectroscopic study of carbonate adsorption to zirconium dioxide sol–gel films from aqueous solutions, Langmuir 13 (1997) 3392–3396.

[41] G. Socrates, Infrared and Raman Characteristic Group Frequencies: Tables and Charts, 3rd ed., John Wiley & Sons Inc., New York, 2001.